

# Flat surface-plasmon-polariton bands and resonant optical absorption on short-pitch metal gratings

W.-C. Tan, T. W. Preist, J. R. Sambles, and N. P. Wanstall

*Thin Film Photonics Group, School of Physics, University of Exeter, Stocker Road, Exeter EX4 4QL, United Kingdom*

(Received 20 November 1998)

The dispersion curves of surface plasmon polaritons (SPP's) on short-pitch metal gratings consisting of an array of narrow Gaussian grooves are calculated. Very flat SPP bands (large band gaps) are observed in the frequency region where the electromagnetic wavelength is much larger than the grating pitch and grating depth. These flat SPP bands originate from the coupled SPP modes localized in the narrow grating grooves. The interaction between SPP modes and free radiation broadens the SPP modes inside the light line and also leads to strong anticrossings wherever the flat SPP bands cross the light line. Excitation of the SPP modes on these zero-order gratings by incident electromagnetic radiation may result in strong resonant absorption. The line shape of the resonant absorption is explained in terms of the radiative broadening and thermal broadening of the SPP modes. [S0163-1829(99)02619-3]

## I. INTRODUCTION

A surface plasmon polariton (SPP) is a fundamental electromagnetic (EM) excitation on a metal-dielectric interface. On a flat metal surface, a SPP mode cannot be directly coupled to by incident radiation because the dispersion curve of the SPP is outside the light cone. On a metallic grating, however, the SPP dispersion splits into bands, just as the electronic states in a periodic potential form into bands, which makes the direct coupling between SPP and radiation modes possible. In effect in-plane momentum is provided by the grating periodicity. It is known that the excitation of SPP modes is the main cause for the optical anomalies on metal gratings, such as resonant absorption,<sup>1-3</sup> large field enhancement,<sup>4</sup> and strong modulation of spontaneous light emission.<sup>5</sup> Clearly the knowledge of the SPP band structure, an inherent property of the corrugated metal surface, is crucial for the understanding of the optical response of metal gratings. The study of SPP dispersion is also important in the context of photonic band structures. Very recently, it has been found that in three-dimensional metallo-dielectric photonic crystals large photonic band gaps can occur at low frequencies where the light wavelengths are much larger than the period of the structure<sup>6</sup> and it is suggested that this is due to strong capacitive coupling between metallic islands. Studying the SPP band structures on metal gratings, which may be considered as simple one-dimensional photonic crystals, may provide substantial insight into the formation of photonic bands in metallo-dielectric photonic solids.

The SPP band structures of metal gratings have been extensively studied in the régime of small pitch to depth ratio.<sup>7</sup> In this régime the SPP can be very well described by perturbation theory which only leads to a band gap at the Brillouin zone (BZ) boundary (the "small-gap" limit) while the dispersion away from the BZ boundary remains unperturbed. Advances in technology permit the manufacture of gratings with nanometer scale pitches and large depth to pitch ratios.<sup>2-4</sup> It has been shown that such structures can have pronounced optical response. Wirgin and Lopez-Rios<sup>3</sup> found experimentally that on a zero-order silver grating containing deep rectangular grooves resonant absorption can occur at

some frequencies accompanied by strong-field enhancement. By modeling a silver surface with nanometer scale roughness as an array of half cylinders embedded in a silver surface, Garcia-Vidal and Pendry<sup>4</sup> found that very localized SPP modes are created, which lead to large-field enhancement. Very recently Sobnack *et al.*<sup>8</sup> studied the scattering of EM waves from zero-order silver gratings at a fixed wavelength and observed that as the grating depth increases a set of reflection minima occur due to the excitation of standing SPP modes localized in the grooves. In contrast to the interest in the optical properties of short-pitch deep metallic gratings, the SPP band structures of such gratings have rarely been studied. As far as we know, the only paper published is that by Laks, Mills, and Maradudin,<sup>9</sup> in which the dispersion relation of SPP's on a metallic grating with a pitch of 50 nm and depth-to-pitch ratio up to 0.6 are calculated by use of an integral method proposed by Toigo *et al.*<sup>10</sup> Their results show that outside the light line very flat SPP bands are formed, but the physical mechanism for the formation of these flat SPP bands was not explained. Furthermore, Laks *et al.* only obtained SPP dispersions outside the light line, therefore their results provide little information about the optical response of a zero-order grating because only the SPP mode within the light cone can couple to incident radiation.

In this paper, we study the dispersion and field distributions of SPP modes on short-pitch zero-order metal gratings. The SPP dispersions both inside and outside the light line are obtained and a clear physical picture for the formation of SPP bands in such structures is proposed. The optical response of the gratings for *p*-polarized (transverse magnetic) light incident in a plane orthogonal to the grating grooves is also calculated over a wide range of frequency and explained in relation to the SPP band structure.

## II. METHOD

Our calculation is based on a method originally proposed by Chandezon *et al.*<sup>11</sup> The essence of the method is to map the curved surface onto a flat plane by the use of a non-orthogonal curvilinear coordinate transformation. The Maxwell's equations are then solved in the new coordinate for both the top medium and the substrate. Matching the tangential components of the fields across the interface, we can cal-

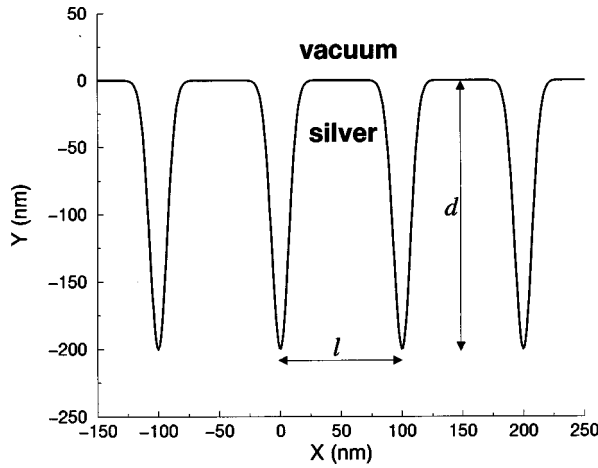


FIG. 1. An example of a grating interface containing an array of identical Gaussian-type grooves ( $l=100$ ,  $d=200$ ,  $w=10$  nm).

calculate the scattering matrix of the interface, which is defined by

$$\begin{pmatrix} C_T^+ \\ C_S^- \end{pmatrix} = S \begin{pmatrix} C_T^- \\ C_S^+ \end{pmatrix}, \quad (1)$$

where  $C_T^+$  ( $C_T^-$ ) is a vector containing the coefficients of upward (downward) going eigenmodes in the top medium and  $C_S^+$  ( $C_S^-$ ) is a vector containing the coefficients of upward (downward) going eigenmodes in the substrate. Since the SPP modes are states bound in the vicinity of the interface, each of them leads to a pole in the scattering matrix.<sup>12</sup> The dispersion relation of the SPP can therefore be obtained by finding the values of frequency  $\omega$  and wave vector  $\mathbf{k}$  that lead to such poles in the scattering matrix. In practice, we calculate the value of

$$P = \sum_{m,n} |S_{m,n}| \quad (2)$$

as a function of  $\omega$  for a fixed  $\mathbf{k}$  along the interface. The SPP frequencies are then given by the peaks in the  $P(\omega)$  curve. Performing the calculation for wave vectors over the whole BZ yields the complete SPP dispersion relation.

We consider a model grating profile defined by

$$y = s(x) = -d \sum_{m=-\infty}^{\infty} \exp\left[-\left(\frac{x-ml}{w}\right)^2\right]. \quad (3)$$

As shown in Fig. 1, such a surface contains an array of identical Gaussian shaped grooves. The advantage of the model is that the depth of the grooves, the width of the grooves and the separation between two neighboring grooves (i.e., the grating pitch) can be controlled independently by adjusting the three parameters  $d$ ,  $w$ , and  $l$ . We assume the top medium and the substrate are air and silver, respectively. The dielectric function of the silver is described by a simple free-electron Drude model,

$$\epsilon_m(\omega) = 1 + \frac{i\tau\omega_p^2}{\omega(1-i\omega\tau)}, \quad (4)$$

where  $\omega_p$  is the plasma frequency and  $\tau$  is the relaxation time of the electrons. In our calculation we have taken  $\omega_p = 1.32 \times 10^{16} \text{ s}^{-1}$  and  $\tau = 1.45 \times 10^{-14} \text{ s}$ ; values for silver.<sup>13</sup>

### III. RESULTS AND DISCUSSIONS

Figures 2(a), 2(b), and 2(c) show the calculated SPP dispersion (thick solid lines) for three silver gratings with grating pitches  $l=50$ , 75, and 100 nm, respectively, at  $k_z=0$  ( $z$  is along the groove direction). All three gratings have the same Gaussian type grooves with  $d=200$  and  $w=10$  nm. For comparison the light line specified by  $\omega = ck_x$  (thin-solid lines) and the dispersion of the SPP on a flat silver surface  $\omega = \omega_{fs}(k)$  (dot-dashed lines) are also plotted. All the SPP bands are quite flat except for the region near the light line, especially for the grating with 100 nm pitch. Figure 3 presents a few  $P(\omega)$  curves for the grating of 100 nm pitch, from which the dispersion shown in Fig. 2(c) is obtained. Because the imaginary part of the dielectric function is much smaller than the real part, SPP modes outside the light cone have a long life time and therefore corresponds to sharp peaks in the  $P(\omega)$  curve. In contrast a mode within the light cone corresponds to a wider peak because it is radiative.

According to simple perturbation theory, band gaps should occur near  $\omega_n = \omega_{fs}(k_n)$ , where  $k_n = n\pi/l$  and  $n = 1, 2, 3, \dots$ , therefore, the number of bands in a given frequency region should strongly depend on the grating pitch  $l$ , so that for all three gratings, there should be no band gap in the frequency region considered. However, Fig. 2 shows that all three gratings have four full bands for  $\omega$  up to  $6.2 \times 10^{15} \text{ s}^{-1}$  despite their very different grating pitches, which clearly indicates that these SPP band structures are beyond the description of perturbation theory.

To understand the physical origin of these SPP bands, we calculate the field distribution of the SPP modes. It is found all the SPP modes considered are related to some kind of standing SPP mode strongly localized in the grating grooves. Figures 4(a) and 4(b) show the amplitudes of the magnetic field of two SPP modes [marked by stars on Fig. 2(c)] for the 100 nm pitch grating. Only the  $z$  component of the magnetic field is plotted because SPP modes are  $p$  polarized. We see that these two SPP modes have very similar field distributions although they belong to different bands and have very different wave vectors. In fact it is found that a SPP mode with a wave vector  $k_x = \pi/l$  in the  $n$ th band and a mode with a wave vector  $k_x = 0$  in the  $(n+1)$ th band always have very similar field distribution, i.e., both have  $n-1$  nodes in a groove [see Figs. 4(a) and 4(b)] suggesting that they originate from the same standing mode. It is also found that the surface charge distributions on the two sides of a groove are antisymmetric for all the modes with  $k_x = 0$  and  $k_x = \pi/l$  (not shown here).

With the help of the field distributions, we propose that the formation of SPP bands shown in Figs. 2(a), 2(b), and 2(c) can be explained by three steps: (1) The narrow groove width results in very strong coupling between surface charges on the two opposite sides of a groove, creating a series of standing SPP modes in each groove. (2) Each of these standing modes is weakly coupled to the corresponding mode in nearest-neighbor grooves and develops into a narrow band. These narrow bands on the  $l=100$  nm grating are

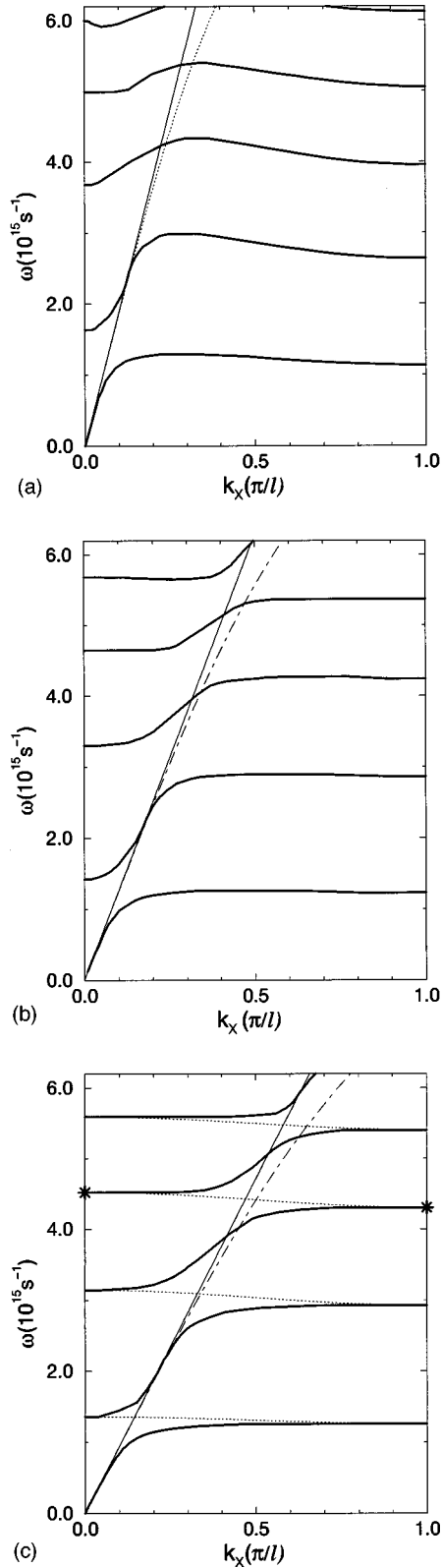


FIG. 2. The calculated SPP dispersion relations (thick-solid lines) for three gratings with grating pitches: (a)  $l=50$ , (b)  $l=75$ , (c)  $l=100$  nm. The three gratings have the same Gaussian shaped grooves ( $d=200$ ,  $w=10$  nm). Also plotted are the light line (thin-solid lines) and the SPP dispersion on a flat silver surface (thin-dot-dashed lines). The four dotted lines in (c) schematically show the narrow SPP bands on the  $l=100$  nm grating derived from the first four standing SPP modes localized in a grating groove.

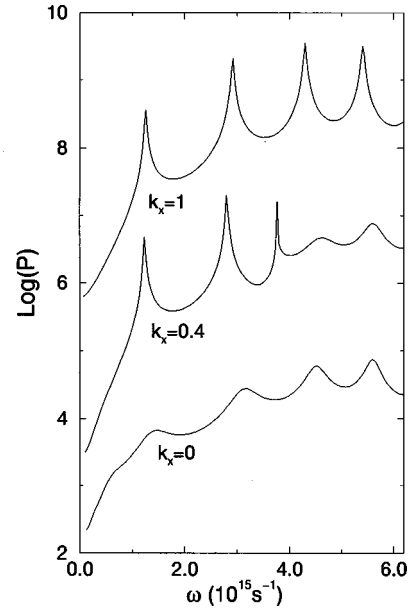


FIG. 3.  $P(\omega)$  curves calculated for the  $l=100$  nm grating at a few  $k_x$  values (in units of  $\pi/l$ ).

schematically illustrated in Fig. 2(c) by thin-dotted lines. (3) The coupling between SPP modes and free radiation leads to strong anticrossings whenever a flat SPP band crosses the light line, therefore resulting in the calculated dispersions. Our detailed arguments are as follows.

First, because of the narrowness of the grooves, surface charges on the two opposite sides of a grating groove are strongly coupled, creating standing SPP modes strongly localized in the groove.<sup>4,8</sup> These coupled SPP modes are similar to the coupled SPP modes in a narrow air gap between two semi-infinite metals.<sup>14</sup> Now, the coupled SPP wave is reflected from the bottom and top of the grooves, producing a zero momentum standing wave. As the width of the air gap is decreased, the coupling increases and the wavelength of this coupled SPP mode becomes much shorter than that of the SPP on an isolated interface. This is why the separations between two neighboring nodes in the field distributions shown in Figs. 4(a) and 4(b) ( $<70$  nm) is much smaller than the corresponding light wavelength ( $\approx 400$  nm).

Considering an isolated groove on an otherwise flat metal surface, the frequency  $\omega_n^0$  of the  $n$ th localized SPP mode can be estimated by requiring that the phase change  $\phi_n$  of the coupled SPP mode along the depth of the groove satisfies

$$\phi_n = \int_{-d}^0 k_c[\omega_n^0, D(y)] dy = \left(n - 1 + \frac{1}{2}\right) \pi. \quad (5)$$

Here  $D(y)$  is the width of the groove, which is  $y$  dependent and  $k_c(\omega, D)$  is the wave vector of a coupled surface plasmon in an air gap of width  $D$  sandwiched by two semi-infinite metals, which is determined by<sup>14</sup>

$$\tanh\left[-(k_c^2 - k_0^2)^{1/2} \frac{D}{2}\right] = \frac{1}{\epsilon_m} \left(\frac{k_c^2 - \epsilon_m k_0^2}{k_c^2 - k_0^2}\right)^{1/2}, \quad (6)$$

where  $k_0 = \omega/c$ .

For a single Gaussian groove with  $d=200$  and  $w=10$  nm on the gratings considered here, this simple estima-

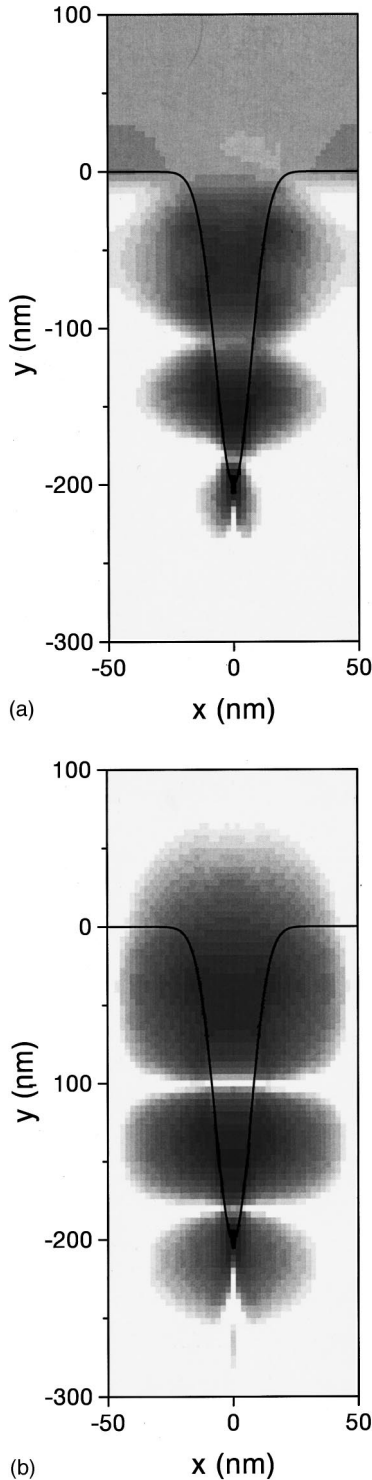


FIG. 4. Distributions of  $|H_z|$  for two SPP modes on the  $l = 100$  nm grating that are marked by stars on Fig. 2(c). (a)  $\omega = 4.53 \times 10^{15} \text{ s}^{-1}$ ,  $k_x = 0$ ; (b)  $\omega = 4.29 \times 10^{15} \text{ s}^{-1}$ ,  $k_x = \pi/l$ . The line represents the grating profile, and regions of high-field intensity are darker.

tion predicts that  $\omega_n^0 = 1.10, 3.07, 4.50,$  and  $5.63 \times 10^{15} \text{ s}^{-1}$  for  $n = 1, 2, 3,$  and  $4$ , respectively. If we take the calculated bands in Fig. 2(c) we see that the  $k_x = \pi/l$  values of the first four bands,  $1.27, 2.90, 4.29,$  and  $5.41 \times 10^{15} \text{ s}^{-1}$ , are closely in agreement with the approximate calculation.

Second, let us now consider the interaction between the

standing SPP modes in different grooves of a grating. The most important interactions are those between the same type of modes in the nearest-neighbor grooves, which are inversely proportional to the product of the dielectric constant of silver,  $\epsilon_m$ , and the separation between nearest-neighbor grooves. Since  $|\epsilon_m| \gg 1$  in the frequency region considered here and the separation between grooves is larger than the groove width, the interactions between standing SPP modes in different grooves can be treated as weak perturbations. It is instructive to consider the standing SPP modes in an isolated groove as the electron levels in an isolated atom, then the formation of SPP bands on a grating is a photonic analogy of the tight-binding model for electron bands in a one-dimensional lattice. Similar to the tight-binding model for electron states, the standing SPP mode with frequency  $\omega_n^0$  will develop into a flat band [as shown by the dotted lines in Fig. 2(c)], which has a simple dispersion

$$\omega_n(k_x) = \omega_n^0 + 2V_n \cos k_x l, \quad (7)$$

where  $V_n$  is a parameter describing the interaction between the  $n$ th standing SPP modes in two nearest-neighbor grooves, which can be estimated by considering the interaction between the surface charges on the two sides of a grating peak. Because the surface charges on the two sides of a groove are antisymmetric, the surface charges on the two sides of a grating peak should be antisymmetric at  $k_x = 0$  and symmetric at  $k_x = \pi/l$ . Noting that the real part of  $\epsilon_m$  is negative we expect  $V_n > 0$  [hence  $\omega_n(0) > \omega_n(\pi/l)$ ], which is in agreement with the calculated results shown in Fig. 2. As the grating pitch increases,  $V_n$  decreases and the SPP bands become flatter, which is clearly seen in Fig. 2. From Eq. (7) we have

$$\omega_n^0 = [\omega_n(0) + \omega_n(\pi/l)]/2. \quad (8)$$

This allows us to calculate  $\omega_n^0$  from the calculated band structures. For the grating with  $l = 100$  nm, Fig. 2(c) gives  $\omega_n^0 = 1.32, 3.05, 4.42,$  and  $5.54 \times 10^{15} \text{ s}^{-1}$  for  $n = 1, 2, 3,$  and  $4$ , which are in very good agreement with the simple estimation from Eqs. (5) and (6) and accord better than the  $k_x = \pi/l$  values from Fig. 2(c).

Third, we have to include the interaction between the flat SPP bands with the continuous spectrum of free radiation. At first sight it seems surprising that the interaction between the flat SPP bands with the free radiation modes spreading over the whole light cone can cause a strong distortion of the flat SPP bands in the vicinity of the light line. The reason is that to enable the coupling between a SPP mode and the free radiation the in-plane wave vectors of the SPP mode and the free radiation, specified by  $k_x$  and  $k_z$ , have to be matched while  $k_y$  does not have to be conserved. The density of states of the free-radiation modes with a given in-plane wave vector  $(k_x, k_z)$  is proportional to  $[\omega^2 - c^2(k_x^2 + k_z^2)]^{-1/2}$ , which is divergent on the light cone  $\omega = c(k_x^2 + k_z^2)^{1/2}$ . Therefore the coupling between the SPP modes with  $k_z = 0$  and the free radiation is strongest near the light line  $\omega = ck_x$ , which leads to strong anticrossings in the SPP band structure whenever the light line crosses the flat bands. Furthermore, because of the interaction with free radiation, the SPP modes within the light cone are no longer bound in the  $y$  direction. They become resonant modes with a finite lifetime as can be seen in

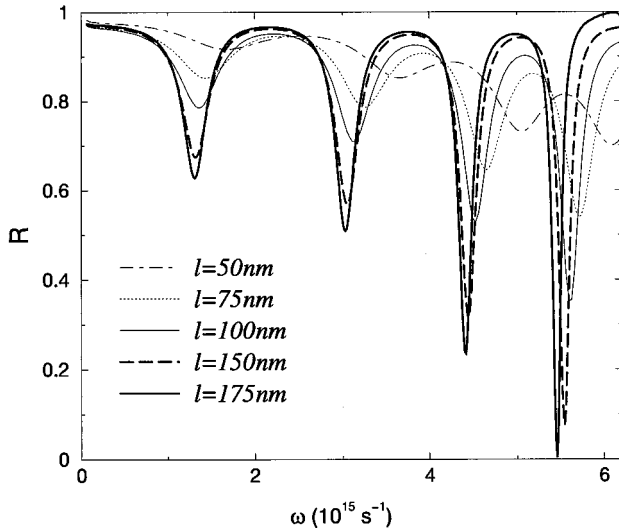


FIG. 5. Reflection coefficients as a function of frequency for  $p$ -polarized normal incident radiation from five gratings consisting of the same Gaussian shaped grooves ( $d=200$ ,  $w=10$  nm) but with different grating pitches:  $l=50$ ,  $75$ ,  $100$ ,  $150$ , and  $175$  nm.

Fig. 3. As discussed above the closer a SPP mode is to the light line the shorter the life time of the mode. Decreasing the separation between the grooves increases the number of grooves per unit length and hence, the percentage of the grooves, consequently this increases the coupling between the SPP modes and the radiation. This in turn broadens the modes.

The SPP bands shown in Fig. 2 can provide a great deal of information about the optical properties of the corresponding grating. For example, if a  $p$ -polarized incident wave has the same frequency and wave vector in the  $x$ - $z$  plane as those of a SPP mode on a grating, it will excite the SPP mode resulting in large-field enhancement in the grooves. Since the dielectric constant of a real metal,  $\epsilon_m$ , has a nonzero imaginary part, the excitation of a SPP mode will lead to resonant absorption and hence, a minimum in the reflection. In Fig. 5, we plot the reflection coefficients of five short-pitch silver gratings as a function of frequency for  $p$ -polarized normally incident light. The five gratings have the same Gaussian shaped grooves as the grating shown in Fig. 1 but they have different grating pitches,  $l=50$ ,  $75$ ,  $100$ ,  $150$ , and  $175$  nm.

Figure 5 shows that in each reflection coefficient curve there are a set of minima. Comparing the curves for the three gratings with  $l=50$ ,  $75$ , and  $100$  nm with the SPP bands shown in Fig. 2, we see that the reflection minima occur at the same frequencies as those of the SPP modes with  $k_x = k_z = 0$  on the corresponding grating. Note, such reflection minima do not exist for  $s$ -polarized incident waves and there are no higher order diffractions since all the three gratings are zero order in the frequency range considered.

The understanding of the formation of the SPP bands can also provide physical insight into the line shape of the reflection minima. Generally the width  $\Delta\omega$  of a SPP mode within the light cone is roughly  $\Delta\omega_{rad} + \Delta\omega_{heat}$ , where  $\Delta\omega_{rad}$  and  $\Delta\omega_{heat}$  are the broadenings corresponding to the radiative loss of energy to the vacuum and the thermal loss of energy to the metal, respectively. The resonant absorption line-shape

related to the SPP mode is determined by the balance of  $\Delta\omega_{rad}$  and  $\Delta\omega_{heat}$ . When  $\Delta\omega_{rad}/\Delta\omega_{heat} \gg 1$  (the over coupling case), the SPP mode only leads to a very shallow and very broad reflection minimum. As  $\Delta\omega_{rad}/\Delta\omega_{heat}$  decreases, the reflection minimum becomes narrower and deeper. The resonant absorption is expected to reach its maximum (where  $R \approx 0$ ) when  $\Delta\omega_{rad}/\Delta\omega_{heat} \approx 1$ . Further decreasing  $\Delta\omega_{rad}/\Delta\omega_{heat}$  narrows the width of the reflection minimum but decreases its depth. Finally, the resonant absorption will disappear as  $\Delta\omega_{rad}/\Delta\omega_{heat} \rightarrow 0$  (the weak-coupling limit).

Figure 5 clearly shows that for a given grating the reflection minima become deeper and sharper as the frequency increases. This is because the radiative damping of the over coupled SPP modes are less at higher frequency. This arises because  $|\epsilon_m|$  of silver decreases rapidly with increasing frequency, the SPP modes at higher frequency can penetrate more easily into the metal, therefore they are more localized in the grooves and the coupling to the radiation is weaker. As a result SPP modes at higher frequency have smaller  $\Delta\omega_{rad}/\Delta\omega_{heat}$  values and therefore lead to narrower and deeper reflection minima. Figure 5 also shows that as the grating pitch increases the reflection minima shift to lower energies and become deeper and narrower, which is again expected from the SPP band structures discussed above. Most interesting is that for the grating with  $l=175$  nm, the reflection minimum at  $5.52 \times 10^{15} \text{ s}^{-1}$  is only 0.003, which indicates that for the corresponding SPP mode the condition  $\Delta\omega_{rad}/\Delta\omega_{heat} \approx 1$  is nearly satisfied.

It should be noted that the so called surface shape resonances recently observed on a lamellar gold grating<sup>15</sup> have a similar physical origin to the resonant absorption shown in Fig. 4. The first resonance in Ref. 15 occurs at a wavelength to groove depth ratio  $\lambda/d \approx 5.5$ , which is slightly larger than the value  $\lambda/d \approx 4$  expected for a very wide groove, while for the 100 nm pitch grating here the first resonance occurs at  $\lambda/d \approx 7$ , reflecting the fact that the coupling between the surface charges on the two sides of a grating groove (500-nm wide) in Ref. 15 is much weaker than that of the narrow grooves studied here.

#### IV. CONCLUSIONS

In conclusion, we have studied the band structures of SPP's on short pitch gratings with narrow and deep Gaussian grooves. Very flat SPP bands (large band gaps) are observed in the frequency region where the EM wavelength is much larger than the grating pitch and grating depth. These flat SPP bands originate from coupled SPP modes localized in the grating grooves, a photonic version of narrow electronic bands developed from tight-binding atomic levels. The coupling between SPP modes and free radiation not only broadens the SPP modes inside the light line but also leads to strong anticrossings wherever the flat SPP bands cross the light line. It is shown that exciting the SPP modes can result in strong resonant absorption of  $p$ -polarized incident EM waves. The frequencies and the width of these flat bands can be easily controlled by the shape (width and depth) of the grooves and the separation between grooves, respectively.

This opens the possibility of engineering the electromagnetic properties of metal surfaces over a wide spectrum ranging from microwave to the visible. Very flat SPP bands correspond to a strong modulation of photonic density of states, therefore short metallic gratings may be used to control the spontaneous light emission of molecules. The simple physical picture for the formation of SPP bands described here

also provides a useful guide for designing more sophisticated metallo-dielectric photonic crystals.

#### ACKNOWLEDGMENTS

The authors are grateful to the Leverhulme Trust for supporting this research, and N.P.W. thanks DERA and EPSRC for financial support.

- 
- <sup>1</sup>R. W. Wood, Proc. R. Soc. London, Ser. A **18**, 269 (1902).  
<sup>2</sup>E. V. Albano, S. Daiser, G. Ertl, R. Miranda, K. Wandelt, and N. Garcia, Phys. Rev. Lett. **51**, 2314 (1983).  
<sup>3</sup>A. Wirgin and T. Lopez-Rios, Opt. Commun. **48**, 416 (1984).  
<sup>4</sup>F. J. Garca-Vidal and J. B. Pendry, Phys. Rev. Lett. **77**, 1163 (1996).  
<sup>5</sup>S. C. Kitson, W. L. Barnes, and J. R. Sambles, Opt. Commun. **122**, 147 (1996).  
<sup>6</sup>D. F. Sievenpiper, E. Yablonovitch, J. N. Winn, S. Fan, P. R. Villeneuve, and J. D. Joannopoulos, Phys. Rev. Lett. **80**, 2829 (1998).  
<sup>7</sup>H. Raether, *Surface Plasmons* (Springer-Verlag, Berlin, 1988); A. A. Maradudin, in *Surface Polaritons*, edited by V. M. Agranovich and D. L. Mills (North-Holland, New York, 1982), p. 405.  
<sup>8</sup>M. B. Sobnack, W. C. Tan, N. P. Wanstall, T. W. Preist, and J. R. Sambles, Phys. Rev. Lett. **80**, 5667 (1998).  
<sup>9</sup>B. Laks, D. L. Mills, and A. A. Maradudin, Phys. Rev. B **23**, 4965 (1981).  
<sup>10</sup>F. Toigo, A. Marvin, V. Celli, and N. R. Hill, Phys. Rev. B **15**, 5618 (1975).  
<sup>11</sup>J. Chandezon, M. T. Dupuis, G. Cornnet, and D. Maystre, J. Opt. Soc. Am. **72**, 839 (1982).  
<sup>12</sup>W.-C. Tan, J. C. Inkson, and G. P. Srivastava, Phys. Rev. B **54**, 14 623 (1996); Semicond. Sci. Technol. **9**, 1035 (1994).  
<sup>13</sup>D. J. Nash and J. R. Sambles, J. Mod. Opt. **43**, 81 (1996).  
<sup>14</sup>E. N. Economou, Phys. Rev. **182**, 539 (1969).  
<sup>15</sup>T. Lopez-Rios, D. Mendoza, F. J. Garca-Vidal, J. Sanchez-Dehesa, and B. Pannetier, Phys. Rev. Lett. **81**, 665 (1998).